Coupling between phonon-phonon and phonon-impurity scattering: A critical revisit of the spectral Matthiessen's rule

Tianli Feng, Bo Qiu, and Xiulin Ruan

Phys. Rev. B **92**, 235206 — Published 16 December 2015

DOI: 10.1103/PhysRevB.92.235206

Coupling between Phonon-Phonon and Phonon-Impurity Scattering: A Critical Revisit of the Spectral Matthiessen's Rule

Tianli Feng, Bo Qiu, and Xiulin Ruan[1,*]

[1]*School of Mechanical Engineering and the Birck Nanotechnology Center, Purdue University, West Lafayette, Indiana 47907-2088, USA*

(Dated: November 29, 2015)

Abstract

The spectral Matthiessen's rule is commonly used to calculate the total phonon scattering rate when multiple scattering mechanisms exist. Here we predict the spectral phonon relaxation time τ of defective bulk silicon using normal mode analysis based on molecular dynamics, and show that the spectral Matthiessen's rule is not accurate due to the neglect of the coupling between anharmonic phonon-phonon scattering τ_a^{-1} and phonon-impurity scattering τ_i^{-1}. As a result, the spectral Matthiessen's rule underestimates the total phonon scattering rate, and hence overestimates the thermal conductivity κ of mass-doped and Ge-doped silicon by about 20-40%. We have also directly estimated this coupling scattering rate, so called coupled five-phonon scattering $\tau_{\text{couple}}^{-1}$, and achieved good agreement between $\tau_a^{-1} + \tau_i^{-1} + \tau_{\text{couple}}^{-1}$ and the total scattering rate τ_{tot}^{-1}.

PACS numbers: 66.70.Df, 61.72.-y, 63.20.kp, 63.20.kg

The spectral Matthiessen's (M's) rule is a general rule to estimate the total spectral scattering rate when multiple scattering mechanisms exist at the same time [1]. In most solids, phonon transport is governed by phonon-phonon scattering $\tau_{a,\lambda}^{-1}$, phonon-impurity scattering $\tau_{i,\lambda}^{-1}$, phonon-boundary scattering $\tau_{b,\lambda}^{-1}$, etc., where λ specifies a phonon mode $\lambda = (\mathbf{k}, \nu)$ with wave vector $\mathbf{k}$ and dispersion branch ν. By adding all of these factors, the spectral M's rule gives the total scattering rate as $\tau_{tot,\lambda}^{-1} = \tau_{a,\lambda}^{-1} + \tau_{i,\lambda}^{-1} + \tau_{b,\lambda}^{-1} + \cdots$. This scattering rate plays a crucial rule in predicting thermal conductivity κ based on the Boltzmann Transport Equation (BTE) $\kappa_z = \frac{1}{V}\sum_\lambda v_{z,\lambda}^2 c_\lambda \tau_\lambda$, where v_z is the projection of the phonon group velocity along the transport z direction, V is the volume, c_λ is phonon specific heat per mode [2], and the summation is done over all the resolvable phonon modes [3]. This approach has been applied to predict the thermal conductivities of isotope-rich semiconductors [4–6], alloys [7–9], nanostructures [10,11], etc [12]. However, as an empirical rule, the M's rule assumes that the scattering mechanisms are independent, which was usually not verified in those calculations employing them. The spectral M's rule has not been examined yet, although the failures of the conventional gray M's Rules, i.e., $\sum \mu_j^{-1} = \mu_{tot}^{-1}$ or $\sum \sigma_j^{-1} = \sigma_{tot}^{-1}$ for electrical transport [1,13] and $\sum \Lambda_j^{-1} = \Lambda_{tot}^{-1}$ or $\sum \kappa_j^{-1} = \kappa_{tot}^{-1}$ for phonon transport [14,15] have been studied extensively, where μ, σ, and Λ are the electron mobility, electrical conductivity and effective phonon mean free path, respectively. Take phonon transport for instance, the correct approach is to first obtain the spectral total relaxation time using the spectral M's rule $\tau_{tot,\lambda}^{-1} = \sum_j \tau_{j,\lambda}^{-1}$, and then derive the thermal conductivity using the Boltamann transport equation (BTE) $\kappa_{tot} \sim \int c(\omega) v_g(\omega) / v_p^2(\omega) \omega^2 \tau_{tot,\lambda}(\omega) d\omega$, where c, v_g and v_p are the phonon specific heat, group velocity and phase velocity, respectively. It can be conveniently shown that only if all the τ_j's have the same ω dependence, one can first use BTE to obtain the partial thermal conductivity due to one scattering mechanism $\kappa_j \sim \int c(\omega) v_g(\omega) / v_p^2(\omega) \omega^2 \tau_{j,\lambda}(\omega) d\omega$, and then use the gray M's rule to obtain the same total thermal conductivity $\kappa_{tot}^{-1} = \sum_j \kappa_j^{-1}$, i.e., the gray M's rule is valid. However, in general the τ_j's have different ω dependencies. Therefore, the failure of the gray M's rule can be expected, while the spectral M's rule has been assumed to be valid all the time. Thus in this letter, our objectives are to 1) predict the spectral phonon scattering rate $\tau_{tot,\lambda}^{-1}$ and thermal conductivity κ without touching the detailed phonon scattering processes or the spectral M's the rule, 2) examine the accuracy of the spectral M's rule and provide physical interpretation and quantitative correction.

We take defective bulk Si as an example and calculate $\tau_{a,\lambda}^{-1}$, $\tau_{i,\lambda}^{-1}$, and $\tau_{tot,\lambda}^{-1}$ in three indepen-

dent ways. $\tau_{a,\lambda}^{-1}$ is obtained by performing the phonon normal mode analysis (NMA) [12,16–21] on pristine silicon, in which only phonon-phonon scattering occurs. $\tau_{i,\lambda}^{-1}$ is calculated from the Tamura's Formulism, and $\tau_{tot,\lambda}^{-1}$ is calculated by NMA on the defective silicon. The spectral M's rule is examined by comparing $\tau_{a,\lambda}^{-1}+\tau_{i,\lambda}^{-1}$ to $\tau_{tot,\lambda}^{-1}$. To examine the accuracy of these scattering rates, we compare the thermal conductivity κ predicted from $\tau_{a,\lambda}^{-1}+\tau_{i,\lambda}^{-1}$ or $\tau_{tot,\lambda}^{-1}$ with that from Green-Kubo method based on MD. The scattering rates $\tau_{a,\lambda}^{-1}$ and $\tau_{tot,\lambda}^{-1}$ were obtained by performing the following NMA on pristine silicon and on defective silicon respectively,

$$q_\lambda(t) = \sum_{\alpha}^{3}\sum_{b}^{n}\sum_{l}^{N_c}\sqrt{\frac{m_b}{N_c}}u_\alpha^{l,b}(t)e_{b,\alpha}^{\lambda *}\exp\left[i\mathbf{k}\cdot\mathbf{r}_0^l\right], \tag{1}$$

$$\Phi_\lambda(\omega) = \left|\mathcal{F}[\dot{q}_\lambda(t)]\right|^2 = \frac{C_\lambda}{(\omega-\omega_\lambda^A)^2+(\tau_\lambda^{-1})^2/4}. \tag{2}$$

Here, $u_\alpha^{l,b}(t)$ is the αth component of the time dependent displacement of the bth basis atom in the lth unit cell, e is the phonon eigenvector, $\mathbf{r}_0$ is the equilibrium position, $\mathcal{F}$ denotes the Fourier Transformation, and $\Phi_\lambda(\omega)$ is called spectral energy density. C_λ is a constant for a given λ. $\Phi_\lambda(\omega)$ is a Lorentzian function with peak position ω_λ^A and full width τ_λ^{-1} at half maximum. By MD simulation the time dependent atomic velocity $\dot{u}$ is obtained and substituted into Eqs. (1) and (2) to obtain the spectral phonon scattering rate τ_λ^{-1}. With this method, we can obtain $\tau_{a,\lambda}^{-1}$ of pristine silicon and $\tau_{tot,\lambda}^{-1}$ of impurity-doped silicon independently. In the evaluation of $\tau_{tot,\lambda}^{-1}$, the intrinsic lattice anharmonicity and the extrinsic impurity are treated as a combined perturbation to the phonon normal modes. This method does not touch the details of the scattering processes or the spectral M's rule.

From the second-order perturbation theory [1,22], Tamura gave the isotope scattering rate by the Fermi's Golden Rule (FGR) [23]

$$\tau_{i,\lambda}^{-1} = \frac{\pi}{2N_c}\omega_\lambda^2\sum_{b}^{n}\sum_{\lambda'\neq\lambda}g_b|\mathbf{e}_b^\lambda\cdot\mathbf{e}_b^{\lambda'*}|^2\delta(\omega_\lambda-\omega_{\lambda'}), \tag{3}$$

where $g_b = \sum_\beta f_{\beta b}(1-m_{\beta b}/\bar{m}_b)^2$ characterizes the magnitude of mass disorder, with β, $f_{\beta b}$ and $\bar{m}_b$ indicating the isotope types, the fraction of isotope in bth basis atom and the average atom mass at the bth basis. Equation (3) is equivalent to $\pi g\omega_\lambda^2 D(\omega_\lambda)/2$ for cubic lattice structures, where $D(\omega)$ is the normalized density of states. The Tamura's Formulism was first derived for the calculation of isotope scattering rate but recently has been applied to many other impurities with bonding change [7–9,24,25]. In the last part of the

letter we study the contribution of the impurity bonding strength to the total scattering rate. In the long wavelength approximation (LWA) [22,23,26], Eq. (3) is reduced to $\sim \omega^4$ relation, $\tau_i^{-1} = \frac{V_c n_c (\Delta m)^2}{4\pi v_g v_p^2 m_c^2}\omega^4$, where V_c is the volume of a unit cell, n_c is the concentration of the impurities, v_g and v_p are the group and phase velocities of phonon, respectively.

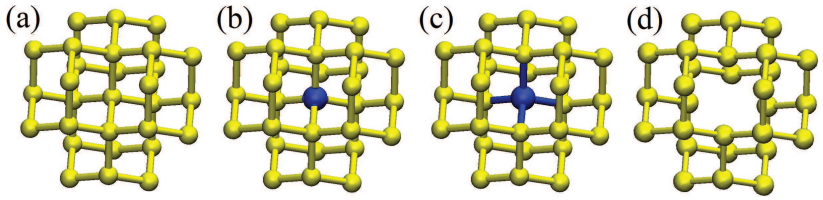

FIG. 1: (Color Online) Sketches of the lattice structures of (a) the pristine c-Si, (b) the mass-doped c-Si (^{m_i}Si-Si), (c) the ^{73}Ge-doped c-Si (^{73}Ge-Si), and (d) the vacancy-doped c-Si (V-Si).

We investigate the pristine c-Si, the mass-doped c-Si (^{m_i}Si-Si), the ^{73}Ge-doped c-Si (^{73}Ge-Si), and the vacancy-doped c-Si (V-Si) bulks [27,28] at classical 300 K with the sketches of the lattice structures shown in Fig. 1. Here the ^{m_i}Si-Si is to substitute some of the original Si atoms with mass m_i while keeping the bonds unchanged. The NMA and the Tamura's Formulism rely on MD simulations and lattice dynamics (LD) calculations, which are conducted in LAMMPS [29] and GULP [30], respectively. All the scattering rates are calculated based on the Tersoff interatomic potential [31]. The domain size and total simulation time are set as $8 \times 8 \times 8$ conventional cubic cells and 10 ns to eliminate the size and time effects [19]. Each time step is set as $\Delta t = 0.5$ fs to resolve all the phonon modes. From the simulation results, it is found that one impurity affects at most the motions of its nearest (2.3 Å) and 2nd nearest (3.8 Å) neighbors because of the approximate tight binding force in silicon. In our simulation, the impurities were randomly distributed with the distance between each of the two defects being larger than 11 Å to ensure the defects do not influence each other. Three or more independent simulations are conducted for each case to minimize the statistical error. In the lattice dynamics calculation we employed a $\mathbf{k}$-grid of $96 \times 96 \times 96$ to obtain results as accurately as possible, since Eq. (1) requires the evaluation of delta functions.

Figure 2 (a) gives the phonon scattering rates of the TA mode in the [100] direction for 0.4% ^{42}Si-Si at classical 300 K. The phonon-phonon scattering rate $\tau_{a,\lambda}^{-1}$ scales as $\sim \omega^2$ at low frequencies, but deviates at higher frequencies. Such a trend was also seen in previous studies [20,32]. The $\tau_{i,\lambda}^{-1}$ calculated from Eq. (3) is found to be exactly the same with

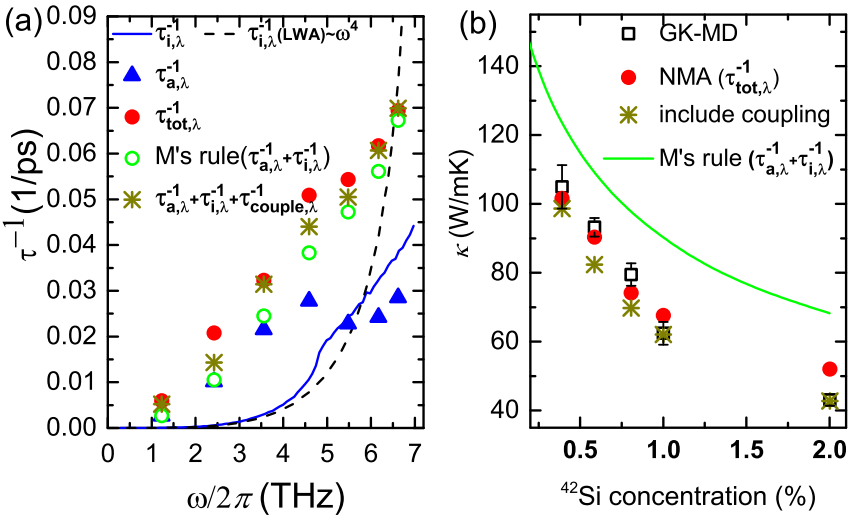

FIG. 2: (Color Online) (a) The phonon scattering rates of the TA mode in [100] direction in pristine c-Si and 0.4% ^{42}Si doped silicon. (b) The thermal conductivity of ^{42}Si-Si calculated from 4 different methods as a function of the ^{42}Si concentration.

$\pi g\omega_\lambda^2 D(\omega_\lambda)/2$ as mentioned above. At low frequency, τ_i^{-1} is about one order of magnitude lower than τ_a^{-1}. As the frequency increases, τ_i^{-1} becomes even higher than τ_a^{-1} due to the increase of the density of states. We also note that the impurity scattering rate obeys the $\sim \omega^4$ relation given by the LWA [dashed black line] for the phonon frequency below 1.5 THz. For higher frequency where phonon wavelength is short and comparable with the defect size, the Rayleigh scattering model breaks down giving way to Mie scattering model and thus the $\sim \omega^4$ frequency dependence gradually fades with increasing frequency [33]. Interestingly, we find that the spectral M's rule, $\tau_a^{-1}+\tau_i^{-1}$ [open green circle], underestimates the phonon total scattering rates [solid red circle] by 10%-50% for different frequencies. To ensure this discrepancy is not due to the different domain sizes used in the NMA and Tamura's Formula, we have performed both the MD simulations and FGR calculations in the domain of 16×16×16 unit cells and the same-size **k**-mesh, respectively. We have found that such discrepancy indeed exists, especially in the mid-frequency range. Actually the impurity scattering rates do not vary much when the **k**-mesh size changes from 96×96×96 to 16×16×16 since the latter is already dense enough to obtain a good phonon density of states. In our work, all the calculations are done based on the same Tersoff potential, and the comparison between the results of different methods is self-consistent. Thus, the

conclusions still hold although the dispersion has discrepancy with experiments.

The thermal conductivity κ as a function of the ^{42}Si concentration at classical 300 K is shown in Fig. 2 (b). The NMA and GK are both based on classical equilibrium molecular dynamics and the same interatomic potential. In our calculation results, their agreement is good (within 5%). As seen in Fig. 2 (b) for the mass doped bulk silicon, the NMA thermal conductivity values (red circles) match excellently with GK values (black squares). For pristine c-Si, our Green-Kubo and NMA methods give consistent thermal conductivity values. In contrast, the κ calculated from the spectral M's rule [green line] has about 20%-40% overestimation. This overestimation has also been observed in the doped silicon with a broad range of mass (28-73) at a concentration of 1%, as seen in Fig. 3.

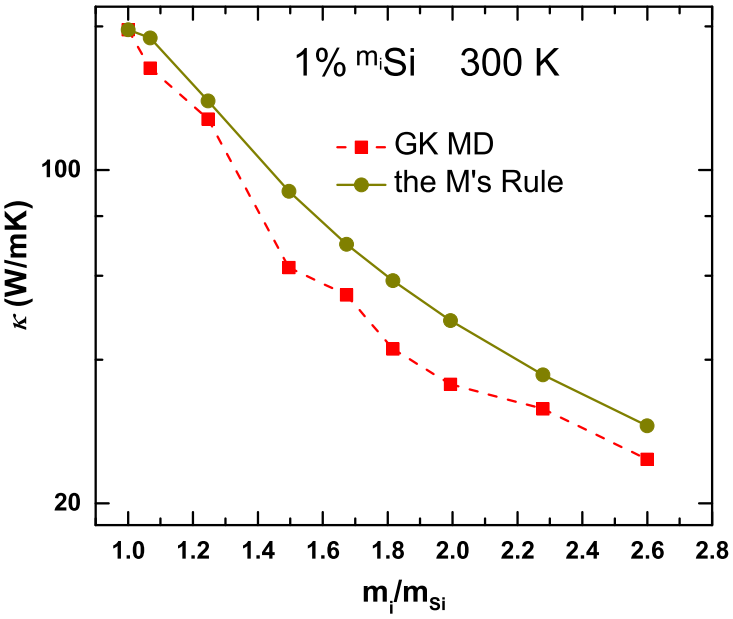

FIG. 3: (Color Online) The comparison of the thermal conductivity calculated from GK-MD and the M's rule for 1% ^{m_i}Si-Si at classical 300 K.

The physical mechanism for the inaccuracy of the spectral M's rule is explored from the second-order perturbation theory [34]. The phonon scattering operator and rate for a defective material are described as

$$H_{\text{scatt}} = H_a + H_i + (H_a + H_i)(E + H_0 + i\varepsilon)^{-1}(H_a + H_i), \tag{4}$$

$$\tau_{tot,\lambda}^{-1} = \tau_{a,\lambda}^{-1} + \tau_{i,\lambda}^{-1} + \tau_{\text{couple},\lambda}^{-1}, \tag{5}$$

where H_0 is the harmonic lattice Hamiltonian, and ε is a positive infinitesimal [34]. The

first two terms H_a and H_i are the perturbation Hamiltonians from intrinsic anharmonicity and extrinsic impurity, leading to intrinsic anharmonic phonon-phonon scattering $\tau_{a,\lambda}^{-1}$ and extrinsic phonon-impurity scattering $\tau_{i,\lambda}^{-1}$, respectively. The former includes the intrinsic 3-phonon, 4-phonon, 5-phonon processes, etc., and the latter involves 2 phonons. The third operator in Eq. (4), which was usually ignored by researchers, represents the coupling between H_a and H_i and may involve 5 or more phonons. To the lowest order of the coupling, the coupled 5-phonon scattering (3 phonons in 3-phonon scattering and the 2 phonons in the impurity scattering) provides additional channels for one mode to scatter to the other mode and thus increases the scattering rate, as shown in Figs. 4 (a) and (b). The detailed sketches for the coupled 5-phonon process are shown in Figs. 4 (c) to (f). Note that this coupled 5-phonon process is different from the intrinsic 5-phonon process which has already been included in the term $\tau_{a,\lambda}^{-1}$. The term "coupling" is used because the transitions occur between the intermediate quantum states of 3-phonon process and impurity-phonon process with detailed sketches shown in Refs. [34,35]. This coupling is calculated by the second-order perturbation theory and is different from the meaning of "interplay" discussed in Refs. [36,37] where the spectral M's rule was still used [38].

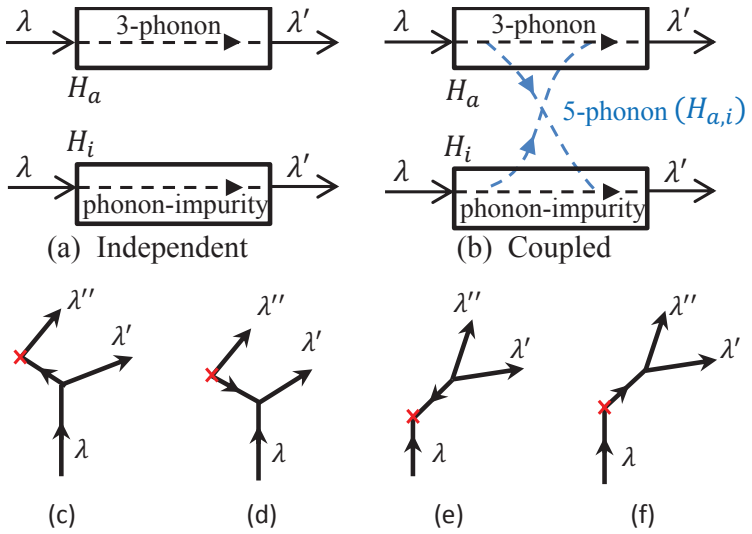

FIG. 4: (Color Online) Brief sketches for illustrating (a) the independent scattering mechanisms and (b) the coupled scattering mechanisms. The sketches of coupling scattering are (c), (d), (e) and (f) with detailed description found in Refs. [34,35]. The × represents the scattering by impurity.

To roughly estimate the contribution of the coupled 5-phonon scattering, we applied the

approximate expression derived by Carruthers from Fermi's Golden Rule [34],

$$\tau^{-1}_{\text{couple},\lambda} = \frac{3g}{4}\left(3\left(\frac{\omega}{\Delta\omega}\right)^2 + \frac{3}{4} + \frac{6\pi\bar{\omega}^4}{\tau^{-1}_{tot,\lambda}\omega_0^3}\right)\tau^{-1}_{a,\lambda}, \tag{6}$$

where $\Delta\omega$ measures "the 'lack' of energy conservation by the intermediate phonons" [34] in the 5-phonon process, and ω_0 is Debye frequency [39]. This coupled 5-phonon scattering rate, however, has never been evaluated before our work. We substitute the τ^{-1}_{tot} obtained from NMA into Eq. (6) to estimate the coupling scattering $\tau^{-1}_{\text{couple},\lambda}$ and check the agreement between $\tau^{-1}_{tot,\lambda}$ and $\tau^{-1}_{a,\lambda} + \tau^{-1}_{i,\lambda} + \tau^{-1}_{\text{couple},\lambda}$. By including the estimated coupling scattering rate $\tau^{-1}_{\lambda,\text{couple}}$, a good agreement is achieved for both τ and κ as seen in Fig. 2. The frequency dependence of $\tau^{-1}_{\text{couple},\lambda}$ in Fig. 2 (a) is explained by Eq. (6) as follows. At low frequencies (1-5 THz) $\tau^{-1}_{\text{couple},\lambda}$ increases with frequency due to the increasing $\tau^{-1}_{a,\lambda}$, while at higher frequencies (6-7 THz), it decreases with frequency since the increasing $\tau^{-1}_{tot,\lambda}$ brings down the third term in the bracket. Physically, at higher frequencies the large density of states allows phonon states to transit into other states quickly by impurity scattering, and thus the intermediate states required in the coupling scattering is probably difficult to produce. Generally, the maximum $\tau^{-1}_{a,\lambda}$ occurs at the mid-frequencies where the phonons have the relatively high $\tau^{-1}_{a,\lambda}$ as well as low density of states.

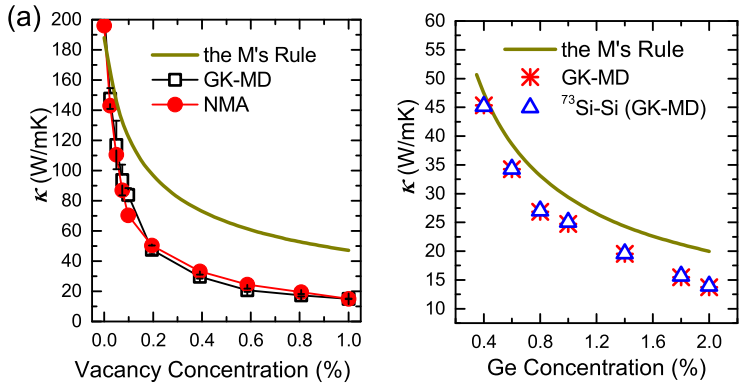

FIG. 5: (Color Online) Thermal conductivity of (a) V-Si and (b) ^{73}Ge-Si calculated from GK-MD, NMA, and the spectral M's rule as a function of vacancy or Ge concentration at classical 300 K. The blue triangles label κ's of ^{73}Si-Si as references.

Figure 5 (a) shows κ of V-Si as a function of vacancy concentration calculated from different methods. We find that even for bond-missing defects our NMA [red circle] presents

excellent agreement with GK-MD [black square], indicating that treating the impurities and anharmonicity as one combined perturbation to calculate total scattering rates is reasonable. The spectral M's rule [yellow line] over-predicts κ of V-Si by about 100-150% at a vacancy concentration of 0.2-1%. The discrepancy comes from two aspects: 1) the spectral M's rule neglects the coupling between phonon-phonon and phonon-defect scattering rates as elaborated earlier, 2) the Tamura's Formulism only captures the scattering by mass disorder while ignoring the bond changes. As for ^{73}Ge-Si shown in Fig. 5 (b), the spectral M's rule over-predicts about 20%-40% of κ. Most of this discrepancy comes from the coupling since we find that ^{73}Ge-Si and ^{73}Si-Si have almost the same thermal conductivity, indicating that Ge-Si bond provides negligible scattering compared to the mass disorder introduced by Ge atoms. In addition, the over-prediction of κ by the spectral M's rule is also seen in the high Ge concentration range [34,40].

For two materials having the same light-doping level ($\tau_{i,\lambda}^{-1} \ll \tau_{a,\lambda}^{-1}$), the coupling strength, defined by $\tau_{couple,\lambda}^{-1}/\tau_{tot,\lambda}^{-1}$ is approximately $1/\tau_{a,\lambda}^{-1}$ and is higher for the higher-κ material which has a lower $\tau_{a,\lambda}^{-1}$. On the other hand, if the doping level is high ($\tau_{i,\lambda}^{-1} \gg \tau_{a,\lambda}^{-1}$), the coupling strength $\sim \tau_{a,\lambda}^{-1}/\tau_{i,\lambda}^{-1}$ is higher for the lower-κ material which has a higher $\tau_{a,\lambda}^{-1}$.

For general materials, the phonon scattering rates as a function of doping concentration is shown in Fig. 6. The coupling scattering rate initially increases rapidly with doping in the light doping regime, and then increases linearly and more slowly in the heavy doping regime. As a result, a maximum of the coupling strength occurs when the system transits from the light to heavy doping. For example, for silicon doped with Ge in our work as shown in Fig. 5(b), the coupling strength increases to 0.4 as the doping level increases to 2%. On the other hand, at the concentration of 50% which is in the alloy-limit, the coupling strength is about $\tau_{couple}^{-1}/\tau_{tot}^{-1} \approx 4\tau_{a}^{-1}/\tau_{tot}^{-1} \approx 4(1/156)/(1/7) \approx 0.2$. Here we used the approximation of $\tau_{couple}^{-1} \approx 10g\tau_{a}^{-1}$ [34] with $g \approx 0.4$ in SiGe alloy and the fact that pristine silicon and SiGe alloy have the thermal conductivities of 156 W/mK and 7 W/mK, respectively. Carruthers et al. hypothesized that this coupled-five phonon scattering caused the over-estimation of for SiGe alloy in early years [34,40], though a quantitative evaluation was not done in their work. The concept of the coupling effect can be extended to all doped material systems, and the general trends should be similar to Fig. 6. For example, the coupling strength in PbTe/Se alloy is estimated to be about 9%, which may account for the overestimation in Ref. [9]. In Ref. [7], Garg *et al.* included the coupling implicitly by calculating the three-phonon scattering rates

in a large SiGe alloy supercell using fully-quantum density functional perturbation theory. Although the 5-phonon processes were implicitly included in prior calculations of the total phonon scattering rates, we are the first to isolate the scattering rate due to 5-phonon processes only.

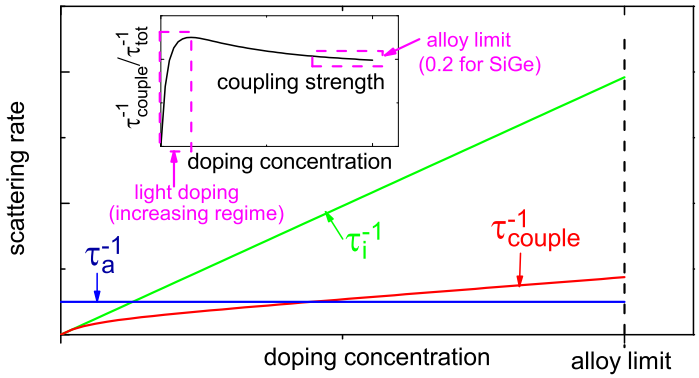

FIG. 6: (Color Online) A sketch to show the scattering rates and the coupling effect (inset) as a function of doping level.

To conclude, without touching the details of the phonon scattering processes, we have used the NMA approach to predict the thermal properties of defective materials more accurately than the spectral M's rule. The spectral M's rule is found to over-predict the phonon relaxation time and thermal conductivity because the spectral M's rule does not take into account the coupling between anharmonic phonon-phonon scattering and impurity scattering. Our results demonstrate one system which has strong coupling between different scattering mechanisms, and for the first time estimate this coupling scattering rates with good quantitative accuracy. Such coupling exists in many different systems of solids, and can be explored for lower κ as well as higher ZT for thermoelectrics.

We would like to thank Prabhakar Marepalli for sharing a part of the Lorentzian fitting codes. Simulations are performed at the Purdue Network for Computational Nanotechnology (NCN). The work is supported by the National Science Foundation (Award No. 1150948). We also thank Dr. Ajit Vallabhaneni, Dr. Frank Brown and Yan Wang for helpful suggestions.

* Electronic address: ruan@purdue.edu

[1] J. M. Ziman, *Electrons and Phonons* (Oxford University Press, London, 1960).

[2] To consistent with the GK method based classical MD simulations, in this work the value of c_λ is taken as k_B under the classical Boltzmann distribution.

[3] J. Turney, E. Landry, A. McGaughey, and C. Amon, Physical Review B **79**, 064301 (2009), ISSN 1098-0121, URL http://link.aps.org/doi/10.1103/PhysRevB.79.064301.

[4] L. Lindsay, D. A. Broido, and T. L. Reinecke, Phys. Rev. B **87**, 165201 (2013), URL http://link.aps.org/doi/10.1103/PhysRevB.87.165201.

[5] L. Lindsay and D. a. Broido, Journal of Physics: Condensed Matter **20**, 165209 (2008), ISSN 0953-8984, URL http://stacks.iop.org/0953-8984/20/i=16/a=165209?key=crossref.fae35963b743f83e18ac9194e2b46a

[6] L. Lindsay, D. a. Broido, and T. L. Reinecke, Physical Review Letters **109**, 095901 (2012), ISSN 0031-9007, URL http://link.aps.org/doi/10.1103/PhysRevLett.109.095901.

[7] J. Garg, N. Bonini, B. Kozinsky, and N. Marzari, Physical Review Letters **106**, 045901 (2011), ISSN 0031-9007, URL http://link.aps.org/doi/10.1103/PhysRevLett.106.045901.

[8] Y. He, I. Savić, D. Donadio, and G. Galli, Physical chemistry chemical physics : PCCP **14**, 16209 (2012), ISSN 1463-9084, URL http://www.ncbi.nlm.nih.gov/pubmed/23060011.

[9] Z. Tian, J. Garg, K. Esfarjani, T. Shiga, J. Shiomi, and G. Chen, Physical Review B **85**, 184303 (2012), ISSN 1098-0121, URL http://link.aps.org/doi/10.1103/PhysRevB.85.184303.

[10] N. Mingo and L. Yang, Physical Review B **68**, 245406 (2003), ISSN 0163-1829, URL http://link.aps.org/doi/10.1103/PhysRevB.68.245406.

[11] P. Martin, Z. Aksamija, E. Pop, and U. Ravaioli, Physical Review Letters **102**, 125503 (2009), ISSN 0031-9007, URL http://link.aps.org/doi/10.1103/PhysRevLett.102.125503.

[12] T. Feng and X. Ruan, Journal of Nanomaterials **2014**, 206370 (2014), ISSN 1687-4110, URL http://www.hindawi.com/journals/jnm/2014/206370/.

[13] Y. Takeda and T. P. Pearsall, Electronics Letters **17**, 1980 (1980), ISSN 00135194.

[14] J. E. Turney, a. J. H. McGaughey, and C. H. Amon, Journal of Applied Physics **107**, 024317 (2010), ISSN 00218979, URL http://link.aip.org/link/JAPIAU/v107/i2/p024317/s1{&}Agg=doi.

[15] M. Luisier, Applied Physics Letters **103**, 113103 (2013), ISSN 00036951, URL http://link.aip.org/link/APPLAB/v103/i11/p113103/s1{&}Agg=doi.

[16] J. A. Thomas, J. E. Turney, R. M. Iutzi, C. H. Amon, and A. J. H.

McGaughey, Physical Review B **81**, 081411 (2010), ISSN 1098-0121, URL http://link.aps.org/doi/10.1103/PhysRevB.81.081411.

[17] A. J. C. Ladd, B. Moran, and W. G. Hoover, Phys. Rev. B **34**, 5058 (1986), URL http://link.aps.org/doi/10.1103/PhysRevB.34.5058.

[18] N. de Koker, Physical Review Letters **103**, 125902 (2009), ISSN 0031-9007, URL http://link.aps.org/doi/10.1103/PhysRevLett.103.125902.

[19] A. McGaughey and M. Kaviany, Physical Review B **69**, 094303 (2004), ISSN 1098-0121, URL http://link.aps.org/doi/10.1103/PhysRevB.69.094303.

[20] A. S. Henry and G. Chen, Journal of Computational and Theoretical Nanoscience **5**, 141 (2008-02-01T00:00:00), URL http://www.ingentaconnect.com/content/asp/jctn/2008/00000005/00000002/art00002.

[21] T. Feng, B. Qiu, and X. Ruan, Journal of Applied Physics **117**, 195102 (2015), ISSN 0021-8979, URL http://scitation.aip.org/content/aip/journal/jap/117/19/10.1063/1.4921108.

[22] P. Klemens, *Solid State Physics*, vol. 7 (Academic Press Inc., New York, USA, 1958).

[23] S.-i. Tamura, Physical Review B **27**, 858 (1983), URL http://journals.aps.org/prb/abstract/10.1103/PhysRevB.27.858.

[24] a. Kundu, N. Mingo, D. a. Broido, and D. a. Stewart, Physical Review B **84**, 125426 (2011), ISSN 1098-0121, URL http://link.aps.org/doi/10.1103/PhysRevB.84.125426.

[25] W. Li, L. Lindsay, D. a. Broido, D. a. Stewart, and N. Mingo, Physical Review B **86**, 174307 (2012), ISSN 1098-0121, URL http://link.aps.org/doi/10.1103/PhysRevB.86.174307.

[26] M. Kaviany, *Heat Transfer Physics* (Cambridge University Press, New York, 2008).

[27] T. Shiga, T. Hori, and J. Shiomi, Japanese Journal of Applied Physics **53**, 021802 (2014), ISSN 0021-4922, URL http://stacks.iop.org/1347-4065/53/021802.

[28] T. Wang, G. K. H. Madsen, and A. Hartmaier, Modelling and Simulation in Materials Science and Engineering **22**, 035011 (2014), ISSN 0965-0393, URL http://stacks.iop.org/0965-0393/22/i=3/a=035011?key=crossref.9b6888a772100db211c7e20bf0534c9

[29] S. Plimpton, Journal of Computational Physics **117**, 1 (1995), ISSN 0021-9991, URL http://www.sciencedirect.com/science/article/pii/S002199918571039X.

[30] J. D. Gale, J. Chem. Soc., Faraday Trans. **93**, 629 (1997), URL http://dx.doi.org/10.1039/A606455H.

[31] J. Tersoff, Phys. Rev. B **39**, 5566 (1989), URL http://link.aps.org/doi/10.1103/PhysRevB.39.5566.

[32] K. Esfarjani, G. Chen, and H. T. Stokes, Physical Review B **84**, 085204 (2011), ISSN 1098-0121, URL http://link.aps.org/doi/10.1103/PhysRevB.84.085204.

[33] P. G. Klemens, Proceedings of the Physical Society. Section A **68**, 1113 (1955), URL http://iopscience.iop.org/0370-1298/68/12/303.

[34] P. Carruthers, Physical Review **125**, 123 (1962), URL http://prola.aps.org/abstract/PR/v125/i1/p123_1.

[35] P. Carruthers, Reviews of Modern Physics **33**, 92 (1961), URL http://rmp.aps.org/abstract/RMP/v33/i1/p92{_}1.

[36] L. Lindsay, D. A. Broido, and T. L. Reinecke, Physical Review B **144306**, 1 (2013).

[37] L. Lindsay and D. a. Broido, Physical Review B **85**, 035436 (2012), ISSN 1098-0121, URL http://link.aps.org/doi/10.1103/PhysRevB.85.035436.

[38] The interplay between isotope scattering and 3-phonon scattering was studied for heavily doped beryllium-VI compounds [36] and boron nitride [37]. There it was illustrated that the highly doped isotopes changed the phonon dispersion relation and further influenced the 3-phonon scattering rate. In their approach, although H_a is modified due to the doping of isotopes, H_a and H_i were evaluated separately and no coupling between them was included. Thus, the spectral M's rule was still used.

[39] Detailed explanation of these parameters are found in Ref. [34], according to which, $\omega/\Delta\omega$, ω_0, and $\bar{\omega}$ are roughly taken as 2, $2\pi\times13$ rad/ps, and $\omega_0/2$, respectively. To roughly estimate the contribution of 5-phonon scattering, the choices of these parameters allow slight changes which will not influence the mangitudes or properties of final results.

[40] B. Abeles, D. Beers, G. Cody, and J. Dismukes, Physical review **125**, 1954 (1962), URL http://prola.aps.org/abstract/PR/v125/i1/p44{_}1.